Dariusz Sokołowski, Wiesław Barnat

Numerical and Experimental Research on the Impact of the Twaron T750 Fabric Layer Number on the Stab Resistance of a Body Armour Package

DOI: 10.5604/12303666.1172090

Faculty of Mechanical Engineering, Department of Mechanics and Applied Computer Science, Military University of Technology,
Kaliskiego 2, 00-908 Warsaw, Poland
E-mail: dsokolowski@wat.edu.pl, wbarnat@wat.edu.pl

Abstract
The aim of the paper was to research how the depth of penetration in dependence on the fabric layer number used in the ballistic package is changed. During the research, the following methodology was adopted: the object of study was Twaron T750 fabric, specially dedicated for use in bulletproof vests. Then a numerical model consisting of 35 layers of fabric was established, from which the following parameters were selected for registration: depth of the knife's penetration, displacement, velocity and acceleration. Then experimental studies were carried out which reflected the numerical model. In the next step a numerical model was validated and variants for the number of layers included in the package were created. The computing environment was commercial software LS-Dyna. Experimental studies were recorded using a super-high-speed camera - PhantomV12. The studies were conducted on the basis of the NIJ Standard -0115.00 norm.

Key words: *stab resistance, body armour, twaron fabric package, numerical model, experimental test.*

Introduction

The aim of this article was to establish the influence of the number of Twaron T750 aramid fibre layers on the penetration value and kinetic energy by means of a stab resistance test. The article is a continuation of a previous paper by the authors, published in Fibres & Textiles in Eastern Europe [1]. The issue of stab resistance is a complex phenomenon influenced by multiple elements, one of which being the number of fabric layers which the protective package is made of [2 - 5, 7, 8]. The number of fabric layers in the body armour package is a value which has a significant influence on the package's surface mass. Consequently determining the exact number of package layers is the most important aspect of the research. Precise examination of the relationship between the number of layers and the penetration value, as well as the kinetic energy, is important because knowledge of this kind may allow for a precise selection of suitable parameters necessary to provide the package with the highest protection effectiveness possible.

Phenomenon description

The basis for the description of the phenomenon was the NIJ Standard-0115.00 norm, which describes the method of carrying out protective package stab resistance tests. The norm was developed in the United States, at the Justice Department. According to the norm, the test was carried out by means of the impact of a free falling sabot equipped with a test knife on a ballistic package placed on deformable ground.

Stab resistance as a physical phenomenon is very complicated due to multiple elements interacting with one another. The most complex is the protective package which, depending on the test, is composed of 17 to 35 Twaron T 750 fabric layers. Each fabric contains hundreds of interweaved roving bundles, of which every single one is, in turn, composed of approximately 2000 aramid fibres of 12 to 15 μm in diameter [6, 9 - 13]. All of the elements mentioned interact with one another. Sole contact is a highly non-linear phenomenon. It is worth mentioning that most of the interacting elements are

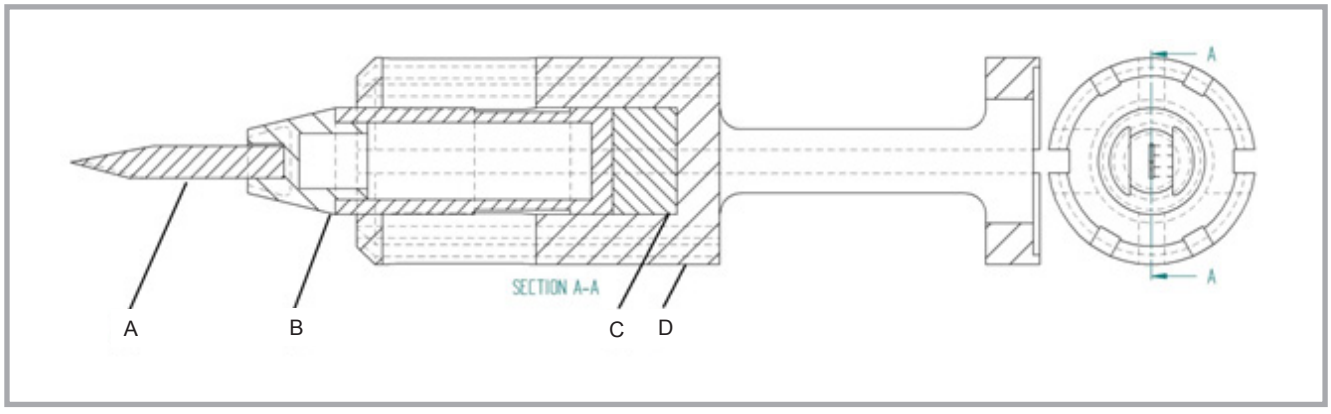

Figure 1. *Sabot cross section with a test knife mounted: A − test knife, B − knife handle, C − dampening element, D − nylon sabot [1].*

Sokołowski D, Barnat W. Numerical and Experimental Research on the Impact of the Twaron T750 Fabric Layer Number on the Stab Resistance of a Body Armour Package. *FIBRES & TEXTILES in Eastern Europe* 2016, Vol. 24, 1(115): 78-82. **DOI:** 10.5604/12303666.1172090

characterised by a different friction coefficient. Among aramid fibres in roving bundles, as well as among roving bundles themselves, there are empty spaces filled with air, which is pushed out during the impact. It is only then that the elements previously separated by the empty space can start interacting. This phenomenon, highly non-linear in itself, introduces the aspect of dampening, which plays a significant role in the phenomenon.

Another element of the system is the sabot unit (***Figure 1***), composed of four independent elements, connected by the contact definition: test knife, handle, dampening element and nylon sabot. Important elements in the sabot unit are the test knife, made of tool steel for cold work, and dampening element made of low-density foam [22].

Figure 2 presents the P1 test knife in accordance with the norm. The knife geometry is significant since it defines the way the knife sinks into the protective package. A P1 knife is the most dangerous because it is characterised by little thickness, which, in turn, results in high energy density at the tip of the blade. At the same time, the thickness helps to prevent the knife's buckling during impact.

Figure 3 presents a simplified phenomenon diagram during the sabot impact on a protective package resting on deformable

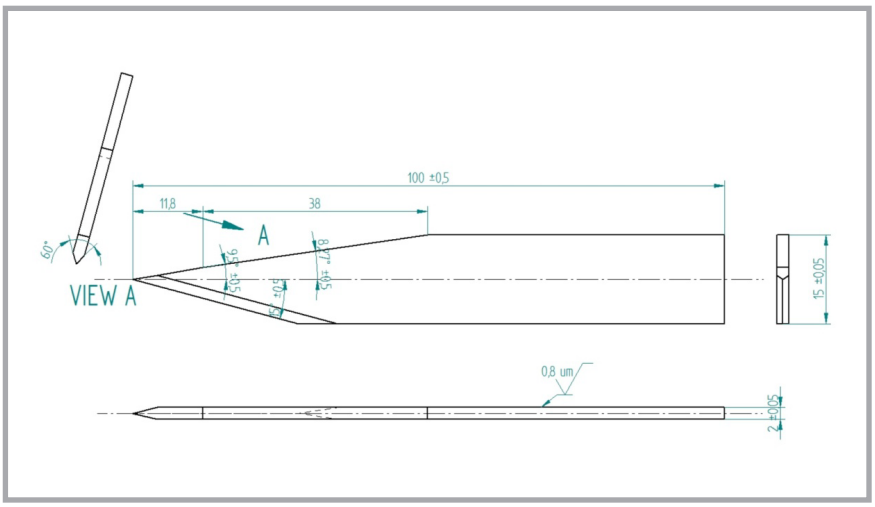

Figure 2. *P1 knife in accordance with NIJ Standard-0115.00 norm [1].*

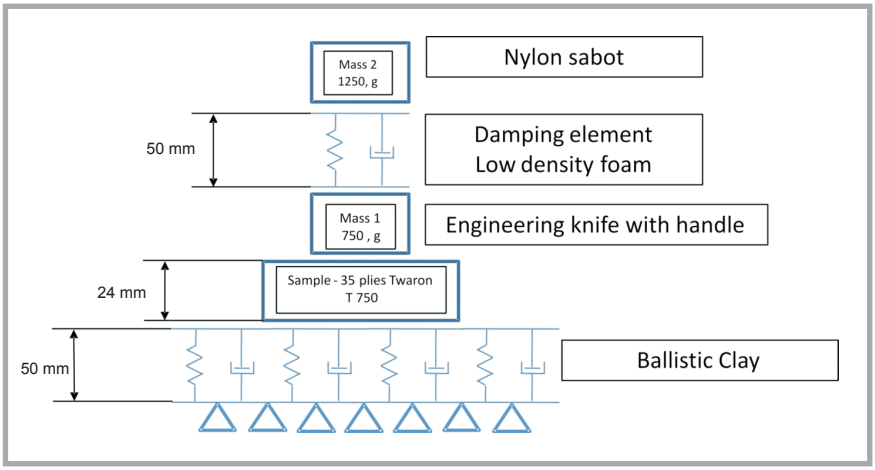

Figure 3. *Simplified system diagram [1].*

Table 1. *Manufacturer's material data sheet [20].*

Style	Linear density, dtexnom	Twaron type	Weave	Set, per 10 cm		Set, per inch		Areal Density		Thickness, mm	Minimum breaking strength, N/5 cm x 1.000		Minimum breaking strength, lb/in x 1.000	
	Warp/Weft	Warp/Weft		Warp	Weft	Warp	Weft	g/m^2	oz/yd^2		Warp	Weft	Warp	Weft
CT T750	3360f2000	2000	Plain	69	69	18	18	460	13.57	0.70	16.50	18.00	1.884	2.056

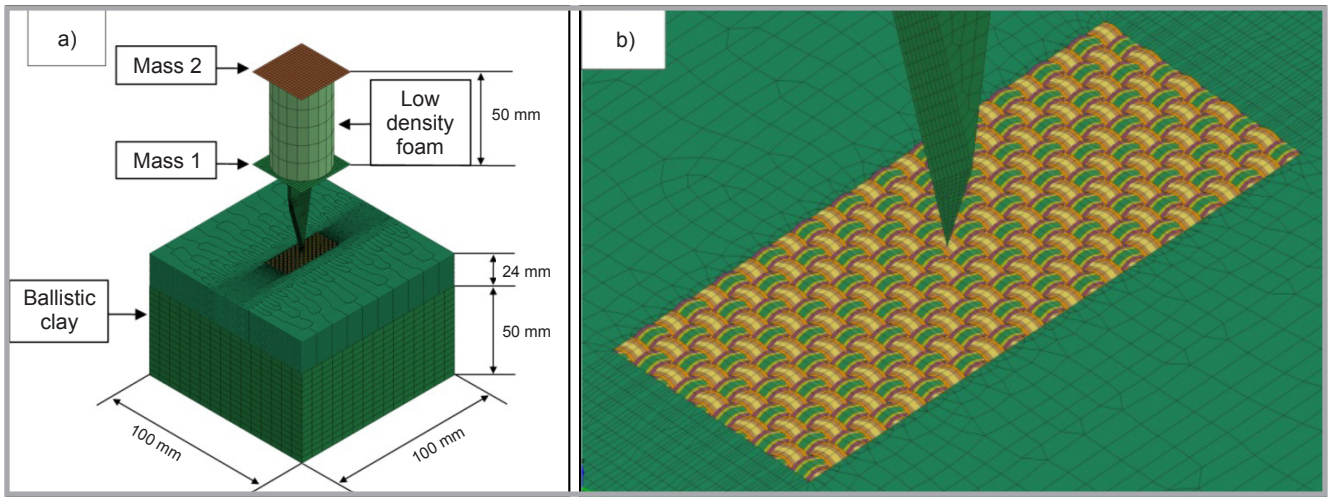

Figure 4. *a) Isoparametric model view (35 layers), b) exact modelling area close-up [1].*

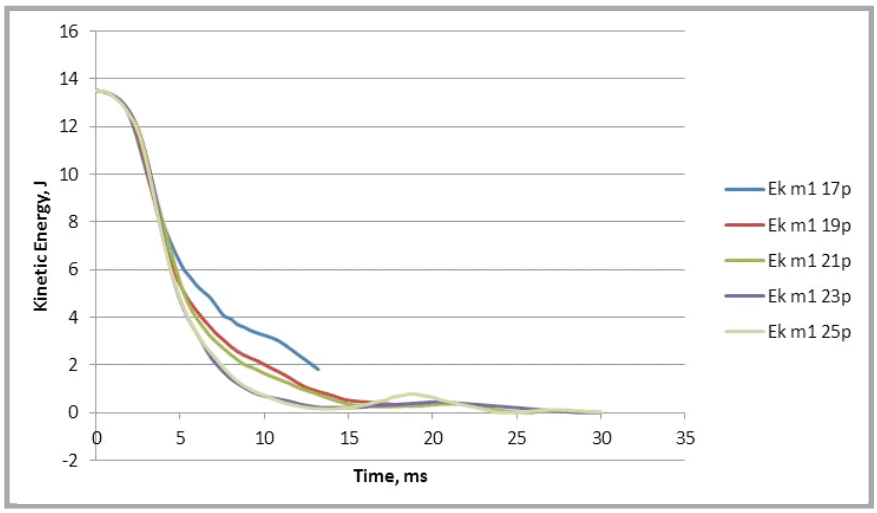

Figure 5. *Kinetic energy of mass 1 for tests from 17 to 25 layers.*

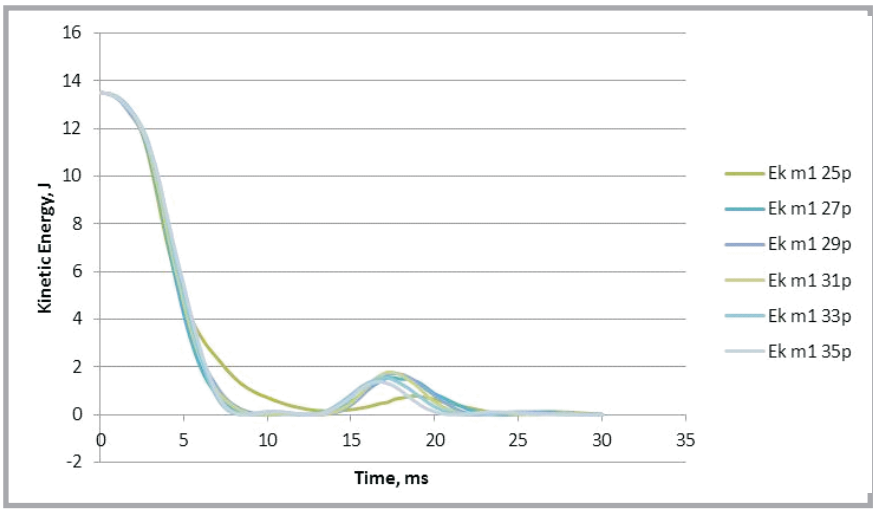

Figure 6. *Kinetic energy of mass 1 for tests of 27 to 35 layers.*

ground. The ground is made of ROMA no 1 clay [21], imitating the human body.

Numerical phenomenon representation

The numerical model representing Twaron T750 fabric is based on the manufacturer's material data sheet (***Table 1,*** see page 79).

Based on the information obtained from the material data sheet, the interlacing geometry was modeled and the roving bundles' thickness selected. The Kevlar fibres' volume coefficient in a bundle was calculated at 50%, which allowed to calculate the alternate Young's modulus and roving bundle density [14]. Element-erosion enhanced orthotropic elastic fabric was used in order to describe the roving bundle fabric model. The parameters of the fabric used in the model are as follows: 57 GPa Young's modulus, 0.001 Poission's ratio, and 0.1 GPa Shear modulus. As the damage parameter, 1550 MPa Principal Stress was used. Roving bundles were reproduced by the use of two-dimensional elements, fully integrable, with a fixed thickness at the level of 0.309 mm. The remaining parameters were discussed in more detail in publication [1].

During deliberations over the issue, 10 numerical models were made, each having, respectively, 17, 19, 21, 23, 25, 27, 29, 31, 33 and 35 layers of Twaron T750 fabric. Each model was charged with identical initial and boundary conditions, namely velocity at a level of 36 J. Translational degrees of freedom were received within the backing material and from sabot elements, excluding the perpendicular direction towards the sabot axis.

A 35-layer model (***Figure 4,*** see page 79) was described in article [1], which was experimentally examined, indicating a significant convergence of results for parameters such as the penetration, course of the velocity curve within the knife's axis, as well as that of the acceleration curve in the knife's axis. Based on this model, its nine variations were established.

Numerical tests' results

In the course of numerical examination, nine protective package configurations were analysed. The packed consisted of different layers: 17, 19, 21, 23, 25, 27, 29, 31, 33 and 35. The experiment was validated based on the 35-layer model.

Based on the experience obtained while examining the 35-layer protective package model, an analysis-ending criterion in the form of a 30 ms boundary time was inferred. The end time was established in this manner because in the case of the 35-layer model the kinetic energy of mass 2 (sabot − 1250 g) was completely transferred to mass 1 (knife + its handle − 750 g). After the 30 ms time, mass 2 changed the velocity turn entirely.

During the research on packages characterised by a low number of layers compared to the reference case (35 layers), it was noticed that the knife's contour entirely exceeds the package's last layer, and the sabot's total energy (mostly of mass 2) is not absorbed.

Based on this, the next calculation-ending condition was inferred in the shape of boundry penetration at a level of 40 mm. Apart from that, the maximal penetration allowed in the norm equals 20 mm.

Figure 5 presents the kinetic energy for mass 1 in models with 17, 19, 21, 23, and 25 layers, respectively. The starting point is 13.49 J energy. It is visible that until the moment in which the energy drops to the level of 8 J, the lines of the chart coincide, which means that the manner of losing energy in all cases remains the same. In the case of 17 layers, the 8 J level is obtained in a time of 4 ms from the beginning of the test. During that time the knife covers a distance of 9.8 mm, which, taking into account the package's thickness of 11.6 mm, constitutes 84.7% of the package's thickness. At this point, the package is punctured almost entirely, which results in a decrease in the package's resistance. This, in turn, causes a slower pace of losing energy.

For the subsequent numbers of layers a similar process can be observed. However, the thickness of the package is bigger, which results in the chart's later separation from the shared line.

An interesting example is provided by the course of energy for 25 layers, because at around 14 ms the kinetic energy is zeroed, and then it begins to rise. A peak is achieved at around 19 ms, at the level of 0.8 J. This is caused by the fact that the velocity of mass 1 is slowed down by the protective package, and next, after some time, mass 1 is accelerated by the constantly falling mass 2. This kind of course is caused by the use of a dampening element between the masses. The function of the susceptible element is to reflect the anatomy of a human-inflicted knife stab. The states between layers 17 and 25 are average .

Figure 6 shows the kinetic energy of mass 1 for models with 27, 29, 31, 33 and 35 layers, respectively. The courses in the above-mentioned examples are very similar as far as the shape is concerned, because in all cases the package thickness was sufficient to consume the mass 1 kinetic energy without puncturing the entire coating in the first moments of time. Differences appear at the moment when mass 2 accelerates mass 1, which is due to different layer thicknesses which are still capable of supporting the knife.

Figure 7 presents the kinetic energy of mass 2 for models with 17, 19, 21, 23 and 25 layers, respectively. In the initial moment of time, there appears a similarity with ***Figure 5*** − the courses of the trend line, up to a particular moment, are very similar. It is due to the fact that mass 2 drops freely until mass 1 slows down to a degree at which it is possible to compress the dampening element and begin transferring its energy to mass 1. This process accelerates in the course of the phenomenon until the moment when the kinetic energy is transformed into internal energy of the system elements. Next the internal energy is once again changed into kinetic energy with a turn opposite to the original one. The course of kinetic energy for the 17 − and 19 − layer cases does not allow the formation of a saddle on the chart, since at that moment the penetration already exceeds 40 mm. Only the 21-layer case allows the formation of a saddle, which is much wider than in the case of 23 and 25 layers. This is related to the stiffness of the package and the number of layers which have been punctured.

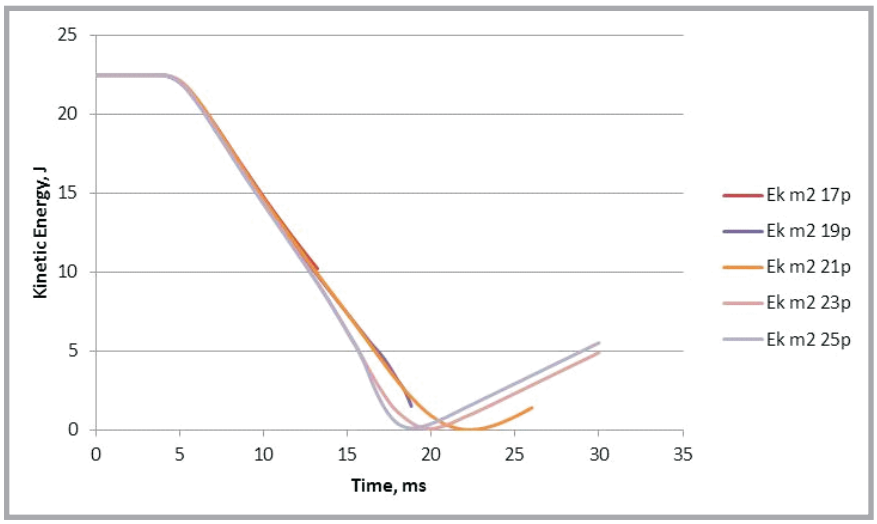

Figure 7. *Kinetic energy of mass 2 for tests of 17 to 25 layers.*

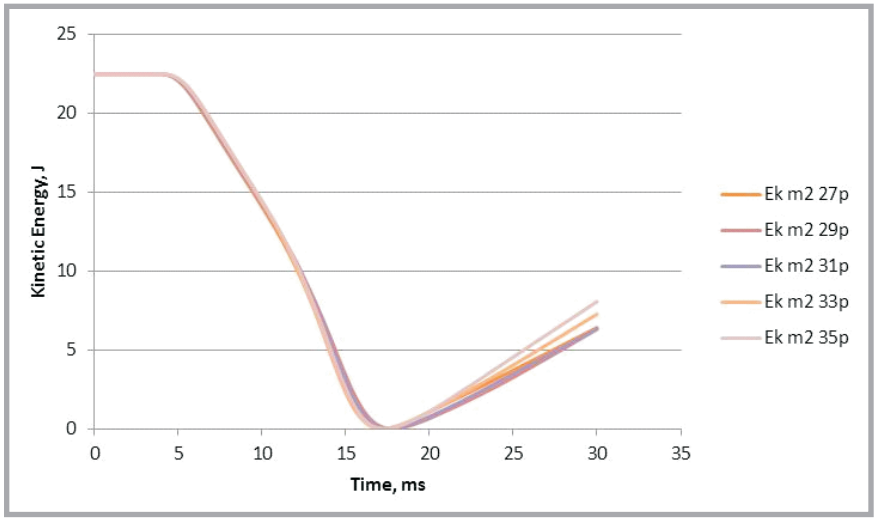

Figure 8. *Kinetic energy of mass 2 for tests of 27 to 35 layers.*

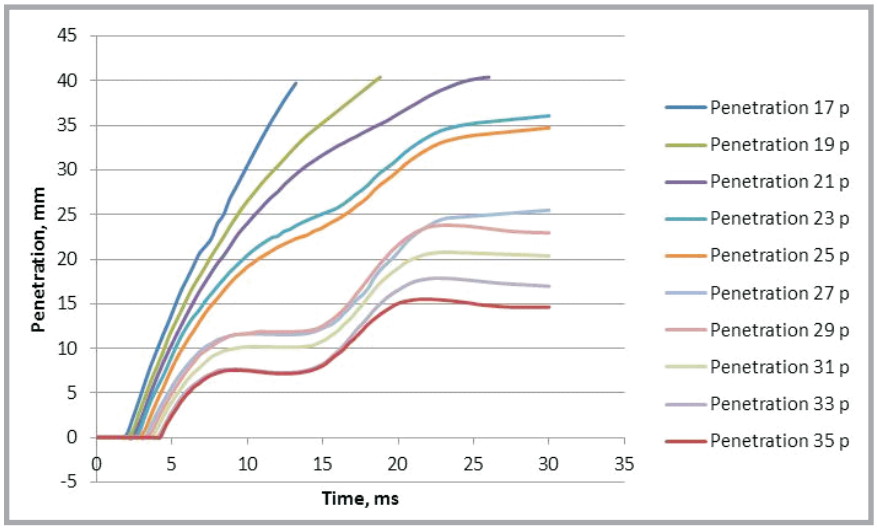

Figure 9. *Tip of knife penetration relative to the last layer of the protective package.*

In ***Figure 8*** one can observe the kinetic energy for mass 2 for models with: 27, 29, 31, 33 and 35 layers, respectively. The course of the trend line for all cases presented remains similar, until the moment of saddle formation (at the moment

of time c.a. 16.4 ms − 17.8 ms). Discrepancies appear only at a later stage. It can be observed that the stiffer the protective package, the bigger the growth of the kinetic energy moving away from mass 2, which results from the amount of energy which has been absorbed by the system. The energy has been absorbed for element erosion and ground deformation.

Figure 9 presents the penetration of the tip of the knife relative to the last layer of the protective package. In the case of the 17-layer model the analysis stopped at the moment (13.2 ms) when the knife reached a 40 mm penetration, which was similar in the cases where the model had 19 (analysis stopped at the moment of time t = 18.8 ms) and 21 layers (analysis stopped at the moment of time t = 26 ms). In the remaining cases the analysis was stopped after 30 ms had passed.

Of interest is the wavy course of the curves resulting from the knife blade's temporary halt, which in turn was a consequence of the slowing down of kinetic energy of mass 1. Subsequently mass 2 begins transferring the kinetic energy to mass 1 and further system penetration takes place until the moment the kinetic energy loses momentum. In the final phase of the trend line course, one can observe a subtle decrease in the penetration value, resulting from mass 2 relieving mass 1, as well as from the package's and ground material's partially resilient effect.

The above-mentioned effects are best observable in the case of a coating containing 35 layers. During the number of layers decreasing, one can see a gradual blurring of the effect due to the fact that the package's stab resistance is diminishing.

Conclusions

The aim of the paper was to examine the relationship between the number of layers in a protective package and the value of penetration of the protective package. It was observed that the number of fabric layers of a protective package is the crucial element in the study of stab resistance.

In the case of the 17-layer model, the analysis stopped at the moment (13.2 ms) when the knife reached a 40 mm penetration, which was similar in cases where the model had 19 (analysis stopped at the moment of time t = 18.8 ms) and 21 layers (analysis stopped at the moment of time t = 26 ms). In the remaining cases the analysis was stopped after 30 ms had passed.

Of interest is the wavy course of the curves resulting from the knife blade's temporary halt, which in turn arose from the slowing down of the kinetic energy of mass 1. Subsequently mass 2 begins transferring the kinetic energy to mass 1 and further system penetration takes place until the moment the kinetic energy loses momentum. In the final phase of the trend line course, one can observe a subtle decrease in the penetration value, resulting from mass 2 relieving mass 1, as well as from the package's and ground material's partially resilient effect.

The above-mentioned effects are best observable in the case of a coating containing 35 layers. During the number of layers decreasing, one can see a gradual blurring of the effect due to the fact that the package's stab resistance is diminishing.

An irregular change between 27 and 25 layers is noticeable, regarding both the penetration value and the characteristics' course. In order to identify the problem, further study on the issue is required.

According to the NIJ Standard – 0115.00 norm, the models with from 31 to 35 layers meet the requirements regarding stab resistance at the first level.

References

1. Barnat W, Sokołowski D, Gieleta R. Numerical and Experimental Research on Stab Resistance of a Body Armour Package. Fibres & Textiles in Eastern Europe 2014; 22, 6(108): 90-96.
2. Miao X, Jiang G, Kong X, Zhao S. Experimental Investigation on the Stab Resistance of Warp Knitted Fabrics. FIBRES & TEXTILES in Eastern Europe 2014; 22, 5(107): 65-70.
3. Olszewska K, Polak J, Zielińska D, Struszczyk MH, Kucińska I, Wierzbicki L, Kozłowska J, Leonowicz M, Wiśniewski A. Textile Multilayered Systems with Magnetorheological Fluids for Potential Application in Multi-Threat Protections. Preliminary Stab - Resistance Studies. FIBRES & TEXTILES in Eastern Europe 2013; 21, 5(101): 112-116.
4. Yu K, Cao H, Qian K, Jiang L, Li H. Synthesis and Stab Resistance of Shear Thickening Fluid (STF) Impregnated Glass Fabric Composites. FIBRES & TEXTILES in Eastern Europe 2012; 20, 6A(95): 126-128.
5. El Messiry M. Investigation of Puncture Behaviour of Flexible Silk Fabric Composites for Soft Body Armour. FIBRES & TEXTILES in Eastern Europe 2014; 22, 5(107): 71-76.
6. Barauskas R., (2007),Multi-Scale Modelling of Textile Structures in Terminal Ballistics, 6th European LS-DYNA Users' Conference
7. Johnson A, Bingham AG, Majewski EC. Establishing the performance requirements for stab resistant Additive Manufactured Body Armour (AMBA). In: The 23rd Annual International Solid Freeform Fabrication (SFF) Symposium, 2012: 297-306.
8. Horsfall I. Stab Resistant Body Armour. Cranfield University, Engineering Systems Department Submitted For The Award Of PhD, 2000.
9. Barauskas R. Multi-Scale Modelling of Textile Structures in Terminal Ballistics. In: 6th European LS-DYNA Users' Conference, 2007.
10. Ha-Minh C, Imad A, Kanit T, Boussu F. Numerical analysis of a ballistic impact on textile fabric. International Journal of Mechanical Sciences 2013; 69: 32–39. DOI: 10.1016/j.ijmecsci.2013.01.014.
11. Nilakantan G, Keefe M, Gillespie JW Jr., Bogetti TA, Adkinson R. A Study of Material and Architectural Effects on the Impact Response of 2D and 3D Dry Textile Composites using LS-DYNA. In: 7*th* European LS-DYNA Users' Conference, 2009.
12. Nilakantan G, Keefe M, Gillespie JW Jr., Bogetti TA. Novel Multi-scale Modeling of Woven Fabric Composites for use in Impact Studies. In: 10*th* European LS-DYNA Users' Conference, 2008.
13. Nilakantan G, Keefe M, Gillespie JW Jr., Bogetti TA, Adkinson R, Wetzel ED. Using LS-DYNA to Computationally Assess the V0-V100 Impact Response of Flexible Fabrics Through Probabilistic Methods. In: 11th European LS-DYNA Users' Conference, 2010.
14. Jones RM. Mechanics of composite materials. Taylor & Francis Inc., 1999.
15. LS-DYNA, Keyword User Manual, 2007.
16. LS-DYNA, Theory Manual, 2006.
17. Livermore Software Technology Corporation, Modeling of Composites in LS LS-DYNA.
18. Kozłowski R, Krasoń W. Numerical simulations in the study of water crossings on the example of a prototype pontoon bridge. Mechanik 2013; 11: 980-981.
19. Krasoń W, Kozłowski R. Dynamic analysis of a multi-mechanism on the example of special floating segments. Biuletyn WAT 2013; LXII, 3: 171-194.
20. Teijin Aramid. Ballistics material handbook, 2012.
21. Sofuoglu H, Rasty J. Flow behavior of Plasticine used in physical modeling of metal forming processes. Tribology International 2000; 33: 523–529.
22. Ouellet S, Cronin D, Worswick M. Compressive response of polymeric foams under quasi-static, medium and high strain rate conditions. Polymer Testing 2006; 25: 731–743.

Received 17.12.2014 Reviewed 13.07.2015